ELSEVIER

Tectonophysics 274 (1997) 253–274

TECTONOPHYSICS

Evolutionary model for the Taiwan collision based on physical modelling

A.I. Chemenda [a,*], R.K. Yang [b], C.-H. Hsieh [b], A.L. Groholsky [c]

[a] *Géosciences Azur, UMR 6526, Université de Nice-Sophia Antipolis et CNRS, 250 Rue Albert Einstein - Sophia Antipolis, 06560 Valbonne, France*
[b] *Institute of Geophysics, National Central University, Chung-Li, Taiwan*
[c] *Moscow State University, Moscow, Russia*

Received 20 January 1997; accepted 20 January 1997

Abstract

2-D and 3-D physical modelling of lithospheric convergence in the Luzon–Taiwan–Ryukyu region is performed with properly scaled laboratory models. The lithospheric model consists of two parts, continental (the Asian Plate, AP) and oceanic (the Philippine Sea Plate, PSP). The oceanic lithosphere has one layer, while the continental lithosphere includes both mantle and crustal layers. The continental margin is covered by sediments. A low-viscosity asthenosphere underlies the lithosphere. The opposing Luzon and Ryukyu subduction zones are initiated by inclined cuts made within the PSP. The subduction/collision is driven by a piston. Pre-collisional intraoceanic subduction along the Luzon and Ryukyu boundaries results in the formation of a transform zone between them, with two tear faults at the ends. The PSP undergoes strong compression along this zone. Subduction of the Chinese margin under the Luzon boundary further increases the compression. Compressive stresses reach the yield limit of the PSP in the arc area, which is a weak zone in the experiments. The plate fails at the western side of the arc along an eastward dipping fault, the Longitudinal Valley Fault. Underthrusting of the frontal wedge of the PSP along this fault results in the closure of the fore arc basin and is then blocked. The PSP fails at the opposite side of the Luzon arc along the westward dipping fault. The failure releases lithospheric compression in this region and results in the initiation of southward-propagating subduction of the PSP under northeastern Taiwan. The incipient subduction zone becomes part of the southeastward-retreating Ryukyu subduction zone, which allows the Okinawa back arc rift to propagate into Taiwan. The Taiwan collision thus includes the following succession of major processes over time, or from south to north: (1) an E–W shortening of the PSP in the Luzon arc; (2) a failure of this plate at the western side of the arc and the formation of the eastward-dipping Longitudinal Valley Fault (the transient plate boundary); (3) a closure of the fore arc basin and a rapid uplift of the orogen; (4) a failure of the PSP at the eastern side of the Luzon arc partly overthrusting the orogen, and the initiation of westward (WN-ward) subduction of the PSP; (5) and finally 'back arc' rifting in the rear of this incipient subduction zone (i.e. in northern Taiwan). All these processes commence with some delay with respect to the preceding ones and propagate southwards.

Keywords: physical modelling; geodynamics; arc–continent collision; continenetal subduction; lithospheric deformation; orogenesis; volcanic arc

* Corresponding author. Tel.: +33 4 9395-4261. Fax: +33 4 9365-2717. E-mail: chem@faille.unice.fr

PII S0040-1951(97)00025-5

1. Introduction

One of the reasons why Taiwan attracts considerable attention from geoscientists is that it lies in an area of ongoing arc–continent collision, which forms an early orogenic stage in many collision belts but which is still poorly understood. What does an arc–continent collision mean in terms of lithospheric mechanics? There is still no quantitative physical model for this process which by definition is caused by subduction of the continental margin (or early continental subduction).

What is the difference between continental subduction and oceanic subduction (or subduction of the oceanic lithosphere)? Why does oceanic subduction not result in the formation of mountain belts, while continental subduction does? In this process, what is the role of the volcanic arc, which is carried by the overriding plate and which defines the difference between an arc–continent and continent–continent collision? These are fundamental questions of geodynamics. They can be resolved only by a combined approach based on the analysis of geological and geophysical data in different regions (corresponding to the different stages and conditions of continental subduction) and on quantitative modelling of continental subduction. Each of these constitutive parts is separately not sufficient to reach the goal, which consists in an understanding of the mechanism of this process. The available geological and geophysical data are far from being sufficient to reconstruct the evolution of the deformation on a lithospheric scale. Modelling itself also cannot provide an unambiguous solution of the problem because of poor knowledge of the boundary and initial conditions. There are also 'internal' technical problems of the modelling, caused by difficulties in the creation of adequate experimental or numerical models, taking into account 3-D aspects of the process, inhomogeneities of the lithosphere, etc. Modelling provides some physically possible scenarios (or puts physical limits on the possible models), which can be tested against and developed based on geological and geophysical data. Taiwan is a very suitable site to test both models and ideas on the mechanical behaviour of the lithosphere during the initial stages of subduction of the continental lithosphere under the plate carrying a volcanic arc (arc–continent collision). The collision in Taiwan is oblique and hence propagating. Therefore, there is opportunity to observe different steps in the process. Taiwan could be an ideal reference region to test the models of early continental subduction, if this process is not complicated by its interaction with the Ryukyu subduction system, including the Ryukyu subduction zone and the Okinawa back arc basin. This interaction makes the situation in Taiwan (or at least in its northern part) essentially three-dimensional, so 3-D modelling is necessary to obtain ideas about the mechanics of complex lithospheric convergence in this region.

In this paper we report results from both 2-D and 3-D physical modelling of the subduction, which adopts but does not reproduce all details of the actual situation in Taiwan. The 2-D experiments were in part previously published by Shemenda (1994) and are summarized here. The 3-D experiments represent the first quantitative 3-D modelling of complex subduction. The results from both 2-D and 3-D modelling are used in combination with geological and geophysical data to develop a first-order evolutionary lithospheric scale model for the Luzon–Taiwan–Ryukyu convergent boundary.

2. Regional geodynamic setting and problems

Convergence of the Philippine Sea Plate (PSP) and the Asian Plate (AP) in the Taiwan area at a rate of >7 cm/yr is accommodated along the opposing Ryukyu and Luzon subduction zones, and directly along the Taiwan orogen (Biq, 1972; Seno, 1977; Fig. 1). Taiwan represents the northern termination of the Luzon subduction zone and started to form only a few to several million years ago, as a result of the collision of the Luzon arc with the Asian continental margin (Biq, 1972; Chai, 1972; Murphy, 1973; Karig, 1973; Wu, 1978; Suppe, 1981; Chi et al., 1981; Barrier and Angelier, 1986; Pelletier and Stephan, 1986; Ho, 1988; Teng, 1990). Due to the oblique orientation of the Luzon arc with respect to the continental margin, the collision in Taiwan (or the subduction of the Chinese margin) propagates southwards, incorporating ever new portions of the Luzon arc (Page and Suppe, 1981; Lewis and Hayes, 1983; Suppe, 1984). The continental subduction is thus more advanced in northern Taiwan and is in its initial stage to the south of Taiwan.

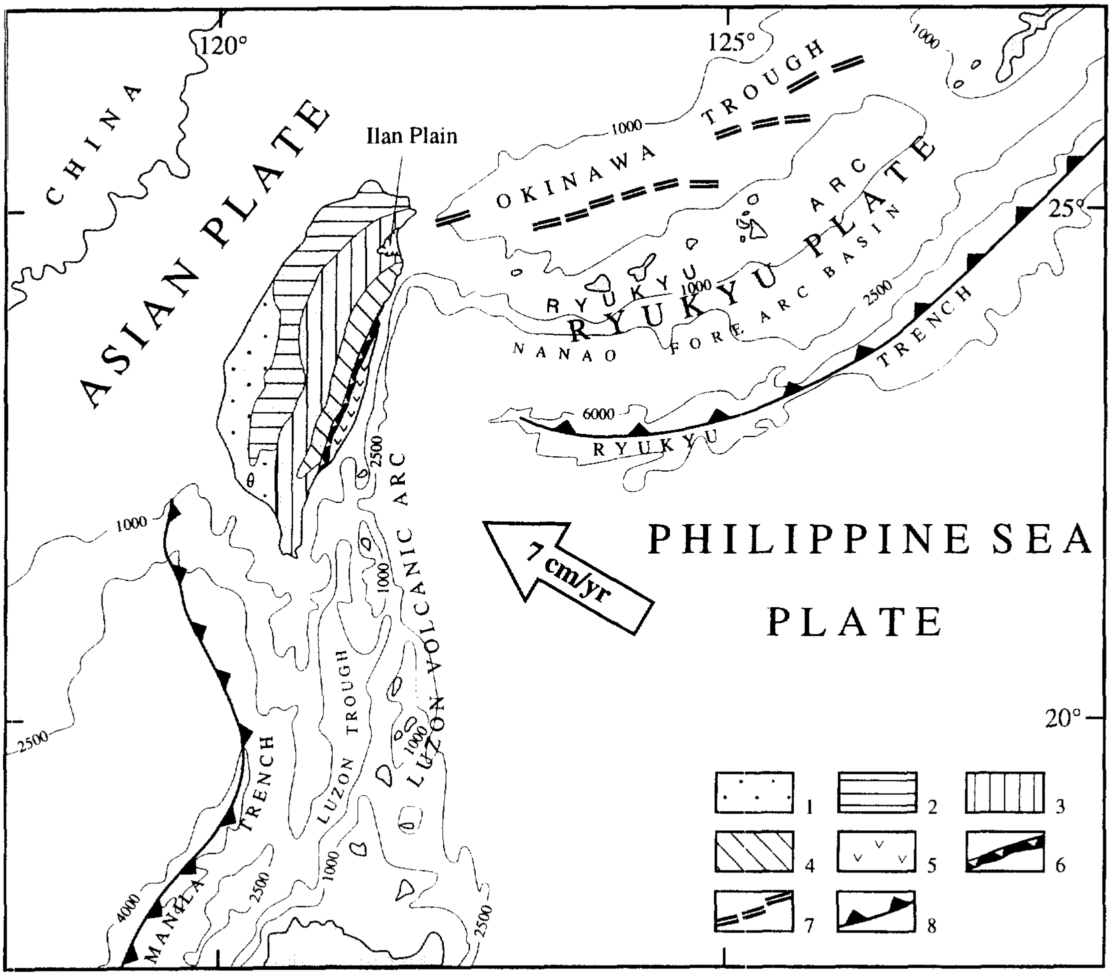

Fig. 1. Geodynamic setting of the Luzon–Taiwan–Ryukyu region (combined and simplified from Ho, 1986, Lundberg et al., 1991 and Sibuet, 1991). *1* = Coastal Plain; *2* = Western Foothills; *3*, *4* = Central Range (*4* = Tananao belt); *5* = Longitudinal Valley with Longitudinal Valley Fault; *6* = Coastal Range (continuation of the Luzon arc); *7* = axis of the Okinawa rift; *8* = subduction zone.

The main body of the Taiwan orogen comprises deformed and accreted sediments of the Chinese continental margin (Chang and Chi, 1983; Ho, 1986; Teng, 1990). At first glance, the accretion mechanism appears to resemble that for the well-investigated accretionary prisms in 'normal' oceanic subduction zones. The only difference seems to be the spatial scale of the accretion, which is much larger in the collisional environment, due to the great thickness of the accreted sediments of the continental margin. However, a more detailed look at the data reveals that the difference is not only the size of the accretionary prism. During the collision a huge accretionary prism approaches the fore arc basin, the Luzon trough, and the volcanic arc, that is the Luzon arc, (Lundberg et al., 1995). Both undergo contraction and uplifting, with the fore arc basin underthrusting the arc along the Longitudinal Valley Fault (Teng, 1990; see Fig. 1). This process is accompanied by local extension within the prism (Angelier et al., 1995; Crespi, 1995; Yu et al., 1995) and exhumation of material from a depth of more than 10 km (Wang Lee et al., 1982; Ernst, 1983). The mechanism for these phenomena is not understood.

The Manila trench and the Luzon arc are a result of the eastward subduction of the AP. Seismicity (Cheng et al., 1995), tomography (Rau and

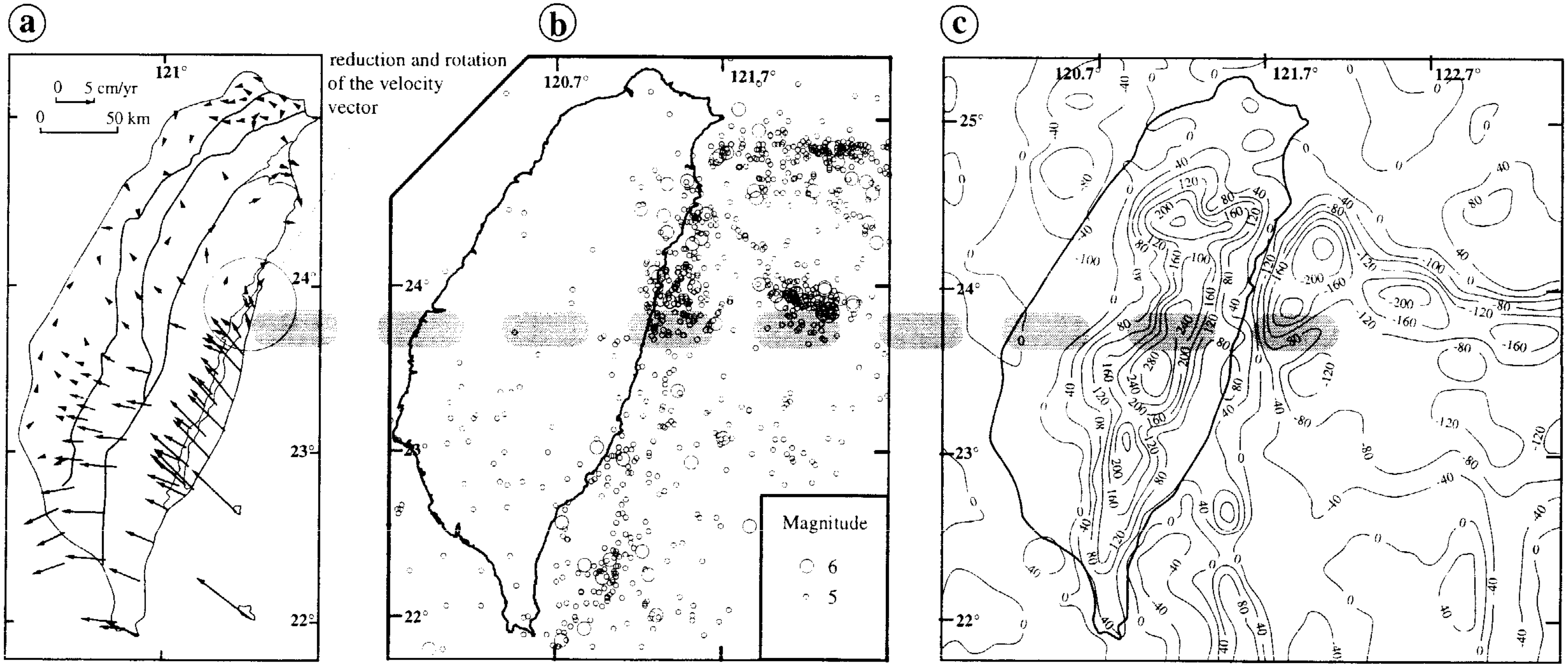

Fig. 2. Three maps characterizing dynamics of the Taiwan region. (a) Velocity field (GPS data) relative to Paisha (Chinese margin) (simplified from Yu et al., 1995) and contours of major faults. (b) Seismicity map of earthquakes with $M_d \geq 5$ located during 1973–1995 by the TTSN. (c) Free-air gravity anomalies map, created by G. C. Tsuei by combining the satellite altimetry data (Geos-3, Seasat and Geosat) and a map by Yeh and Yen (1991) for Taiwan. (See text for explanation of dashed shaded line throughout the figure.)

Wu, 1995), marine geophysical (Lundberg et al., 1991), and GPS (Yu et al., 1995) data show that this subduction continues to the north under southern Taiwan. Southern Taiwan represents thus an active accretionary structure where convergence is accommodated along active thrust faults both onland and offshore, as is attested to by the GPS data (see Fig. 2a). The western front of active deformation (front of the accretionary prism) is traced to about 23°N (Lundberg et al., 1991) (see Fig. 1). A regional plate convergence at near 5 cm/yr is taken up to the east of southern Taiwan (see Fig. 2a) by a shortening of the PSP in the Luzon arc–fore arc area. Deformation in this area is also manifested by active seismicity (Fig. 2b). The AP subduction is slowing down to the north, with a considerable part of the convergence (near 3 cm/yr) being taken up by the Longitudinal Valley Fault (Figs. 1 and 2a), which is a major east-dipping lithospheric fault. Northern Taiwan is also a young accretionary structure, made up of the accreted series of the Chinese margin (Teng, 1990). GPS data (Fig. 2a) reveals that there is almost no shortening in northern Taiwan. Seismicity is also considerably lower in this area. It is concentrated in a narrow zone along the northeastern margin of Taiwan (Fig. 2b). Subduction of the AP under northern Taiwan has thus ceased, but the rapid convergence between the AP and the PSP continues. Where is this convergence accommodated? Certainly, somewhere to the east of Taiwan, most probably along the above-mentioned seismicity concentration zone, along the northeastern margin of Taiwan which attests to the intensive ongoing lithospheric deformation. Focal mechanisms indicate a WN-shortening in this area (Cheng et al., 1995). What is the style of this deformation? One can suppose that the Longitudinal Valley Fault (LVF) extends offshore further to the north and takes up this shortening. However, GPS data show that convergence along northern onland termination of this fault has completely ceased (Fig. 2a). There is no reason to suppose that it increases again along an offshore extension of the LVF. Thus, the convergence is taken up further to the east, within the PSP. The mechanism for lithospheric deformation in this area could be plastic shortening of the PSP, which sooner or later must be followed by its failure, and the formation of a new convergent plate boundary. Probably this has already happened. The concentration of seismicity near northeastern Taiwan could correspond, in this case, to the incipient subduction of the PSP under Taiwan as suggested by Shemenda et al. (1992) and Shemenda (1994).

GPS measurements (Fig. 2a) as well as seismicity data (Cheng et al., 1995) show that instead of E–W shortening, northern Taiwan undergoes some extension in this direction. The extension affects not only the upper layers, but most probably the whole lithosphere, resulting in rifting within the Ilan Plain, which is a continuation of the Okinawa rift (Barrier and Angelier, 1986; Sibuet, 1991; Fig. 1). The Okinawa trough is a typical active back arc basin (Letouzey and Kimura, 1986; Sibuet, 1991) formed due to the southeastward retreat of the Ryukyu trench (the whole Ryukyu subduction zone). This process does not seem to be related to or caused by the Taiwan collision. The retreat of the Ryukyu zone could be due either to gravitational sinking of the PSP (pull force) or excess (superhydrostatic) pressure exerted by the mantle upon the surface of the subducted PSP (Shemenda, 1994). Either of these mechanisms reduce the pressure between the subducting PSP and the overriding Ryukyu Plate. Low pressure causes non-isostatic subsidence in the fore arc area. The subsidence, on the one hand, forms a fore arc basin (Fig. 1), and on the other hand, causes an intensive negative gravity anomaly associated with the basin (Fig. 2c). This anomaly continues up to Taiwan and then turns to the south, reaching maximal value, of about 200 mGal, in the corner zone. This extremely intense anomaly certainly results from the interplay between the Ryukyu subduction system and the collision in northern Taiwan, which causes a reorganization of plate boundaries. This interplay is manifested by the propagation of the Okinawa rift into northern Taiwan (Fig. 1) and the above-mentioned bending near Taiwan of the gravity minimum associated with the Ryukyu zone. The Benioff zone marking the PSP subducted under the Ryukyu arc, also seems to extend under northern Taiwan (Wu, 1978) up to section 2 in Fig. 3. This observation may lead to the conclusion that the Ryukyu subduction zone would continue to the west, onland, in northeastern Taiwan. However, there is no geological or geophysical evidence of such a continuation, except the Benioff zone already mentioned. What is the origin of this Benioff zone? How can the Okinawa rift 'intrude' into a

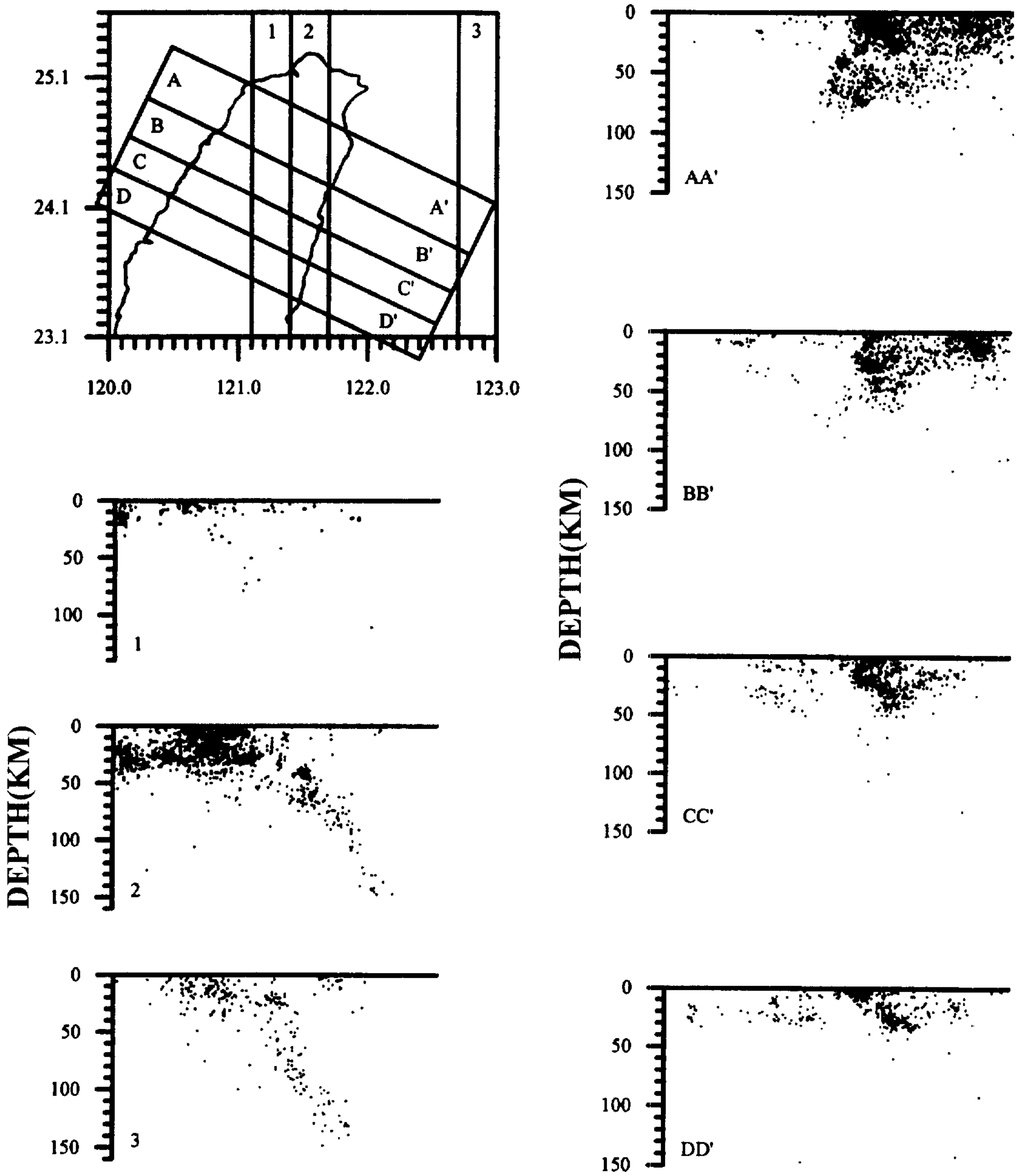

Fig. 3. Vertical seismicity sections for magnitude $M_L \geq 3$ (updated from Wang et al., 1994).

northern Taiwan which has resulted from very recent compressional accretionary tectonics? What are the present plate boundaries between the Luzon and Ryukyu subduction zones and their evolution? In this paper we try to address these and other problems of regional geodynamics based on physical modelling.

3. 2-D mechanics of arc–continent collision

The 2-D physical modelling of this process was reported by Shemenda (1994). In this section we summarize the results of these and other similar experiments conducted within the set-up presented in

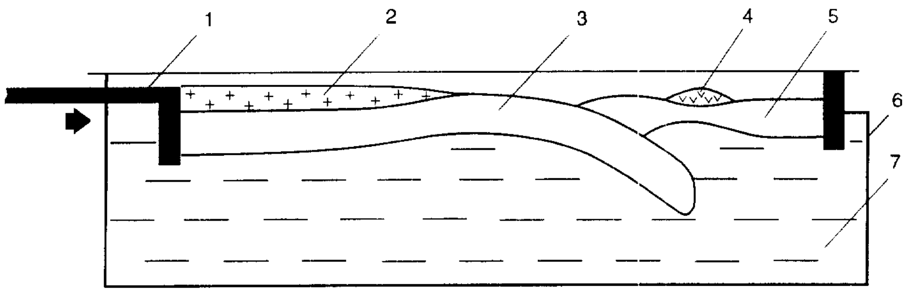

Fig. 4. Scheme of 2-D modelling: *1* = piston; *2* = continental crust; *3* = oceanic part of the subducting plate (the same material as the mantle layer of the continental lithosphere); *4* = volcanic arc (the same material as the continental crust); *5* = overriding plate; *6* = tank; *7* = low-viscosity asthenosphere. All the lithospheric layers possess plastic properties with strain-weakening rheology and are made of hydrocarbon compositional systems (see Shemenda, 1994, for the details).

Fig. 4. The modelling shows that the stress state of the lithosphere in the subduction zone depends on the density contrast $\Delta\rho = \rho_l - \rho_a$ (ρ_l is the average density of the subducting lithosphere and ρ_a is the asthenospheric density), Shemenda (1993). At $\Delta\rho > 0$ the overriding plate can undergo extension (during subduction) in a direction perpendicular to the plate boundary. If $\Delta\rho < 0$ the overriding plate undergoes compression, which grows with absolute value of $\Delta\rho$, or with decreasing ρ_l at ρ_a = const. Such a compressional regime can characterize both oceanic and continental subduction. The thickness of the low-density crust increases across the continental margin from the ocean to the continent, which reduces the average density of the lithosphere. Therefore, subduction of the continental margin causes a progressive increase in lithospheric compression. If both the subducting and overriding plates are strong and able to withstand the growing compression without failure, then the continental crust can subduct to a great depth (more than 150 km), resulting in the formation of a high mountain belt (Chemenda et al., 1995, 1996). If one of the plates is weak enough, then it will fail, resulting in a jump of the subduction zone to the place of failure and a cessation of the subduction of the continental lithosphere. The potential place of failure (the weakest zone) is the volcanic arc weakened due to a number of factors, such as induced convection in the mantle, magmatic activity (presence of the magma chambers and channels), and increasing water content, which provides the weak wet rheology of the overriding plate in the arc area. In the experiments we produced weakening of the lithosphere under the arc by its thinning (Fig. 4). During subduction of the continental margin the lithosphere under the arc undergoes flexural subsidence and then plastic shortening when compressive stress reaches the yield limit of the lithosphere (Fig. 5b). The plastic deformation occurs through the shearing along two systems of slip lines (Fig. 5b) and produces a gradual failure of the material, which results in a macro failure of the lithosphere. Failure occurs along one of two potentially possible directions (faults) coinciding with two systems of slip lines. The modelling revealed two principal factors which control the orientation of the resultant fault: (1) the average distance L between the interplate surface and the weak zone (volcanic arc), and (2) the interplate frictional stress τ_n (Fig. 5a). During the subduction of the continental margin at small τ_n, the overriding wedge undergoes uplifting, which is a kinematic effect caused by the increasing height of the subducting plate surface (the dynamic effect is an increase in the lithospheric compression). If the distance L is small, this uplift makes failure of the weak zone along the fault dipping under the arc to the west (to the left in Fig. 5) kinematically more favourable. If L is larger than a certain critical value L_c, then failure occurs along the opposite direction (as shown in Fig. 5c), due to the flexure and clockwise rotation (in cross-section) of the frontal segment of the overriding plate as shown in Fig. 5b. The L_c value depends on the distribution of interplate pressure and the flexural rigidity of the overriding plate. In the experiments $L_c \approx 2H$ (H is the plate thickness shown in Fig. 5a). Interplate friction produces the opposite effect. If τ_n is high and distance L is small, the overriding wedge is dragged down as a

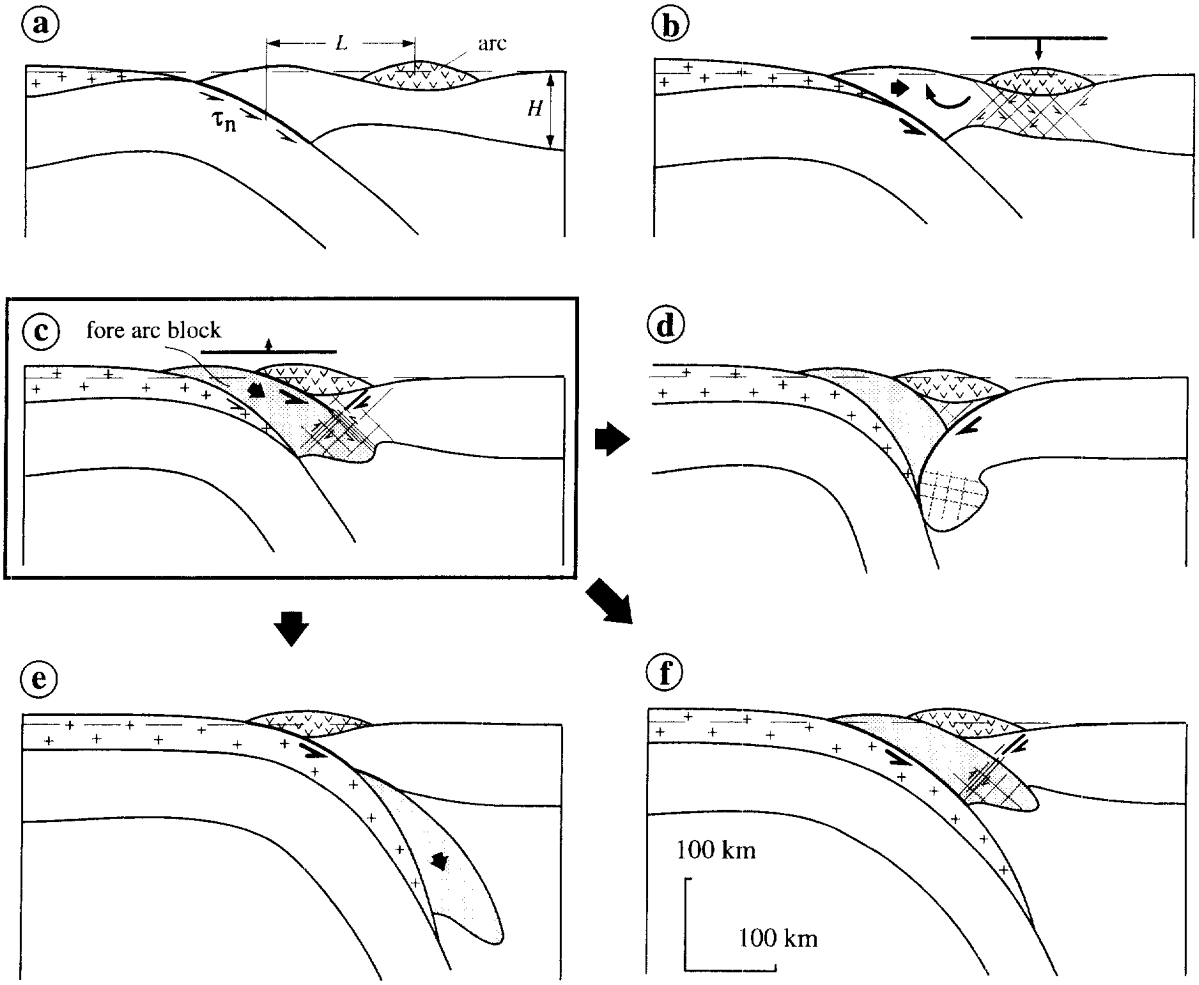

Fig. 5. Summary of the results from 2-D modelling of arc–continent collision. (a to c) Initial stages of the 'collision'. Three possible scenarios are shown for lithospheric deformation after stage (c): (c) → (d), (c) → (e), and (c) → (f), which depend on the model parameters (see text for explanations). Vertical arrows in (b) and (c) show directions of vertical movements.

rigid block, causing failure along the fault, dipping to the east. A larger L allows flexural bending and counter-clockwise rotation (in cross-section) of the wedge under the frictional force which defines the opposite dipping of the fault. Which of these two physically possible modes of failure corresponds to the Taiwan situation is difficult to predict because there are no constraints on the value of τ_n, nor on the distribution of the interplate pressure. As will be seen below, the geological situation in this region seems to fit the case in Fig. 5c, corresponding to a failure along an eastward-dipping fault, followed by underthrusting of the fore arc block under the arc. The fore arc block can subduct into the mantle either completely (Fig. 5e), if it has a mantle density (or oceanic origin), or partly if the density is lower. In the latter case, there are two possible options: a renewed subduction of the continental lithosphere (Fig. 5f), or a failure of the overriding plate at the opposite side of the arc along another potential failure surface, resulting in subduction reversal (Fig. 5d). This again depends (in the experiments) on L and τ_n, as well as on the strength, strain weakening, thickness of the overriding plate, and density of the mantle layer of the subducting plate. All these parameters are not well constrained for the prototype (nature). However, the choice between the physically possible options in Fig. 5d–f can be easily made based on the GPS data. As pointed out above, these data show that the eastward subduction of the AP under northwestern Taiwan ceased, with convergence between the AP and the PSP being taken up offshore of northeastern Taiwan. Such a scenario fits only Fig. 5d.

The evolution of the arc–continent collision in Taiwan in a 2-D approximation can thus be presented successively as shown in Fig. 5a–d. These evolutionary stages may also correspond to the present-day sections through the Luzon–Taiwan boundary, starting off southern Taiwan where oceanic subduction is still going on (Fig. 5a) up to northern Taiwan (Fig. 5d) where continental subduction has reached its most advanced stage. This model does not take into account the process of accretion of sediments of the Chinese margin, and most importantly, the 3-D nature of plate convergence in the Taiwan area. Below we present the results of the simplified 3-D physical modelling of this process.

4. Experimental set-up and similarity criteria

The experimental technique and the facilities for 3-D experiments are similar to those for 2-D modelling. Fig. 6 shows a scheme of the experimental model. The lithosphere is initially continuous, consisting of two parts, the continental part (the Asian Plate) and the oceanic part (the Philippine Sea Plate). The oceanic lithosphere is one layer, while the continental lithosphere has two layers, the mantle (made of the same material as the oceanic lithosphere) and the crust. The transition zone from the continent to the ocean (the continental margin) is covered by sediments (Fig. 6). All the lithospheric layers possess plastic properties and are made of the hydrocarbon compositional systems as in the 2-D experiments. The crust and the mantle layer both have the same yield limit and are characterized by a strong strain weakening. The sediments are considerably weaker and more ductile. The lithosphere is underlain by a low-viscosity asthenosphere which in the experiments is pure water. Convergence is driven by a piston moving at a constant rate throughout the experiment. To initiate subduction along the Luzon and Ryukyu subduction zones, we made two opposite dipping cuts through the whole thickness of the oceanic lithosphere, as shown in Fig. 6.

The following similarity criteria are met by this modelling (Shemenda, 1994):

$$\sigma_l/(\rho_l g H_l) = \text{const};\ \sigma_l/\sigma_c = \text{const};\ \sigma_l/\sigma_s = \text{const};$$
$$\rho_l/\rho_a = \text{const};\ \rho_l/\rho_s = \text{const};\ \rho_l/\rho_c = \text{const};$$
$$H_l/H_c = \text{const};\ H_m/H_c = \text{const};\ d/H_c = \text{const};$$
$$Vt/H_l = \text{const} \qquad (1)$$

where σ_l, and ρ_l are the yield limit under normal loading, and the density for both the oceanic lithosphere and the mantle layer of the continental lithosphere; ρ_c and σ_c are the density and the yield limit of the crust, respectively; ρ_a is the asthenospheric density; H_l, H_c, and H_m, are the thicknesses of the oceanic lithosphere, the continental crust, and the mantle layer of the continental lithosphere, respectively; d, ρ_s and σ_s are the width, the density, and the yield limit of the continental margin sediments; V is the rate of subduction; t is the time; g is the acceleration of gravity.

The following parameter values for the prototype (nature) and the model satisfying criteria (1) are assumed. For the original (prototype): $\sigma_l^o = \sigma_c^o = 2.1 \times 10^8$ Pa; $\sigma_s^o = 10^7$ Pa; $\rho_l^o = \rho_a^o = 3.3 \times 10^3$ kg/m^3; $\rho_c^o = \rho_s^o = 2.84 \times 10^3$ kg/m^3; $H_l^o = 5 \times 10^4$ m; $H_c^o = 3.4 \times 10^4$ m; $H_m^o = 5.2 \times 10^4$ m; $d^o = 3 \times 10^5$ m; $V^m = 7$ cm/yr. For the model: $\sigma_l^m = \sigma_c^m = 28$ Pa; $\sigma_s^m = 1.3$ Pa; $\rho_l^m = \rho_a^m = 1 \times 10^3$ kg/m^3; $\rho_c^m = \rho_s^m = 0.86 \times 10^3$ kg/m^3; $H_l^m = 2.2 \times 10^{-2}$ m; $H_c^m = 1.5 \times 10^{-2}$ m; $H_m^m = 2.3 \times 10^{-2}$ m; $d^m = 13 \times 10^{-2}$ m; $V^m = 5 \times 10^{-5}$ m/s. 1 min in the model corresponds to about 4×10^4 years in nature. Superscripts 'o' and 'm' denote the original and the model, respectively. For more experimental details see Shemenda (1994).

5. Results of 3-D modelling

Fifteen experiments were conducted, with different cut orientations (proto-Luzon and Ryukyu subduction zones), and deep structure of the continental margin (its width and layer thicknesses). Fig. 7 shows a typical result. Compression of the lithospheric model initiates subduction along the inclined cuts and their rapid propagation towards each other (Fig. 7b). The overriding edge of the Philippine

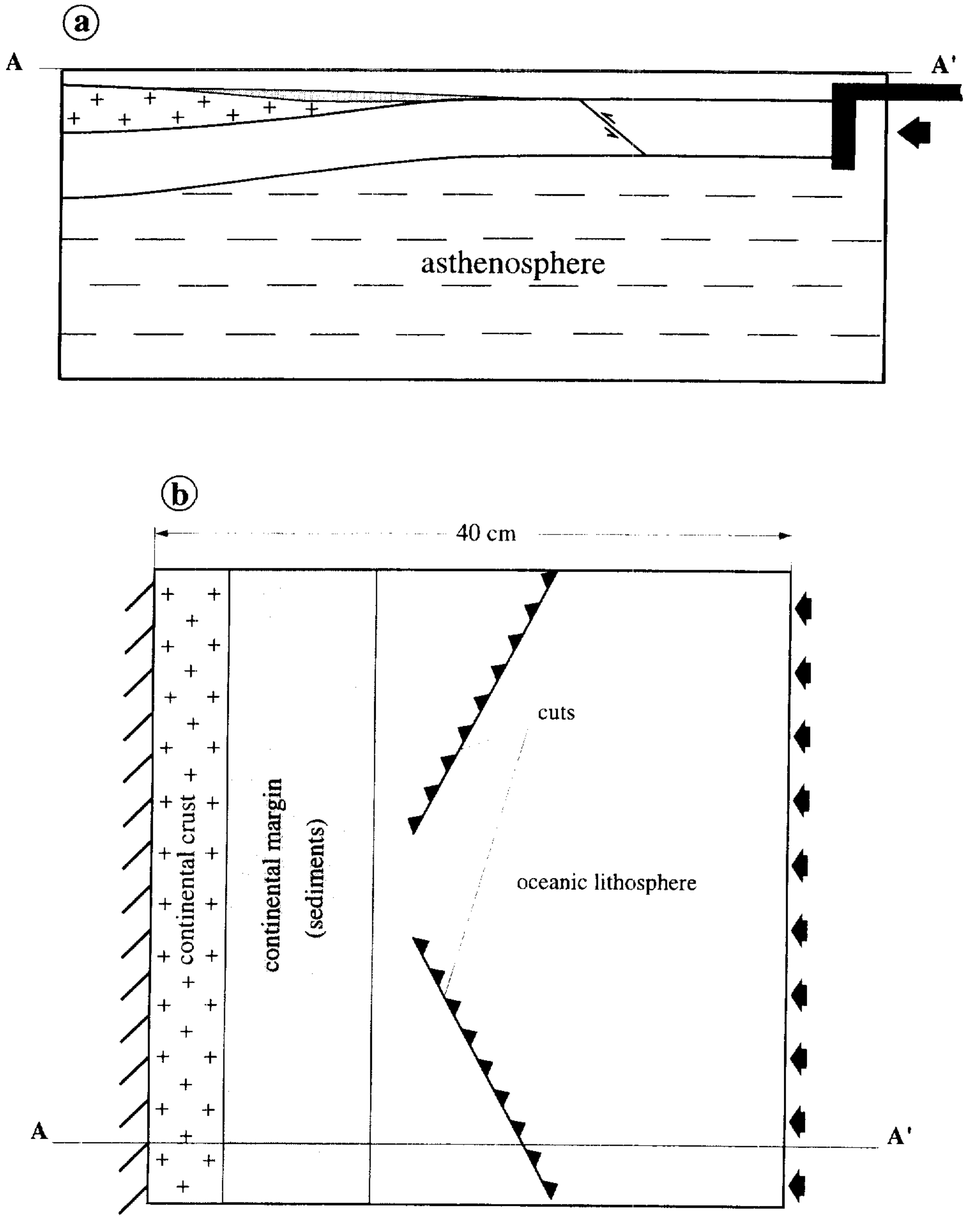

Fig. 6. Scheme of 3-D modelling. (a) Cross-section of the experimental model. (b) Plan (section *A–A'* corresponds to (a)).

Sea Plate (PSP) approaches the continental margin along the Luzon segment of plate boundary, while the Ryukyu zone remains in the same position. The PSP then begins to override the continental margin, partly scraping off the sediments of the margin to form an accretionary prism (Fig. 7c). Another (lower) part of the sedimentary layer is dragged down along the interplate zone. The western tip of the Ryukyu boundary segment merges with the Luzon segment and bends clockwise, forming a transform zone between the two segments (Fig. 7d). The deformation of the Asian margin propagates southwards due to the oblique orientation of the Luzon zone with respect to the margin. The 'collision' is thus

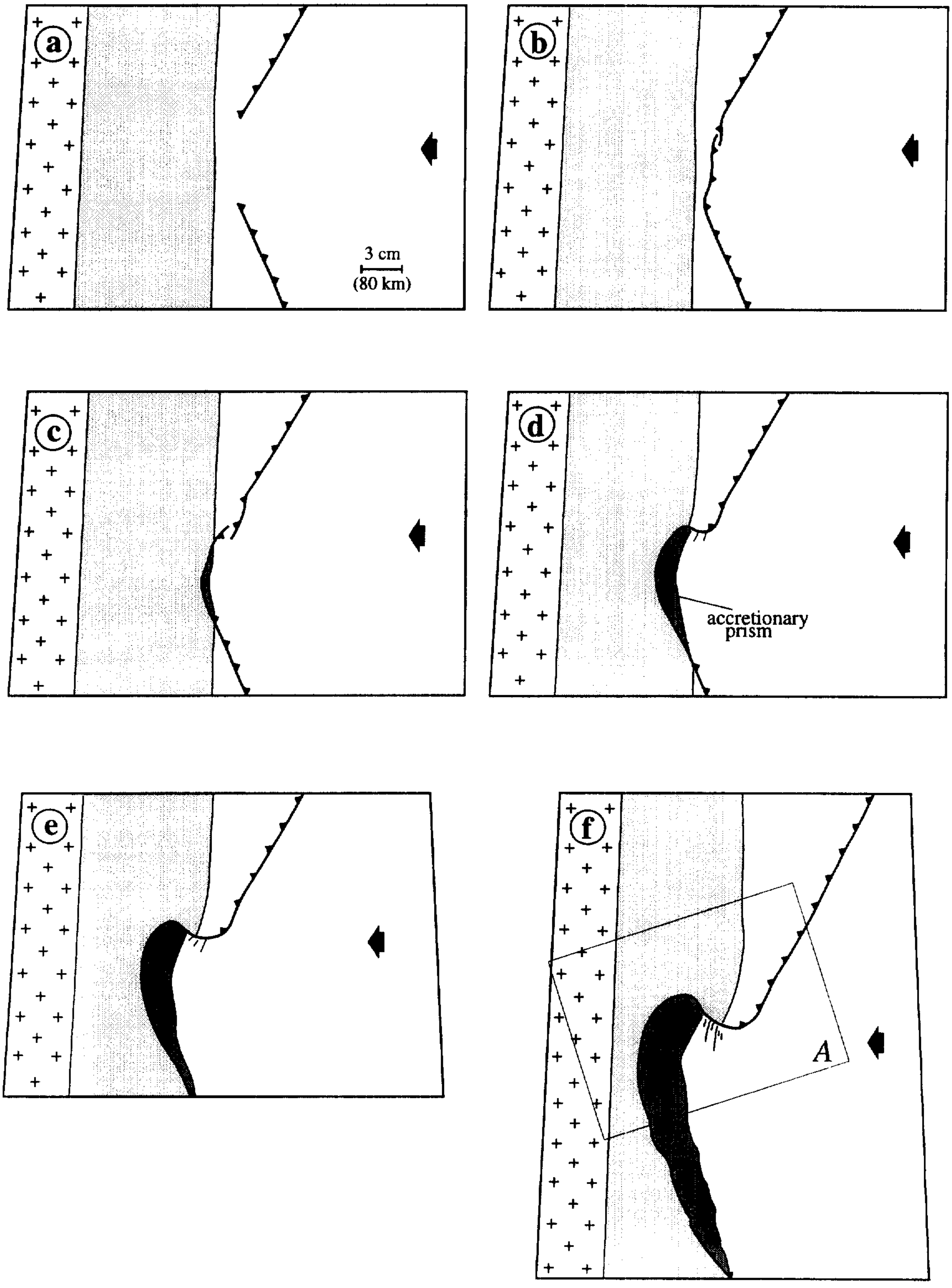

Fig. 7. Successive stages of the model deformation in plan (exact drawing copies of the experimental photos). The photos have been taken slightly oblique to the model surface. Photo of area A (f) is presented in Fig. 9. Shading patterns as in Fig. 6.

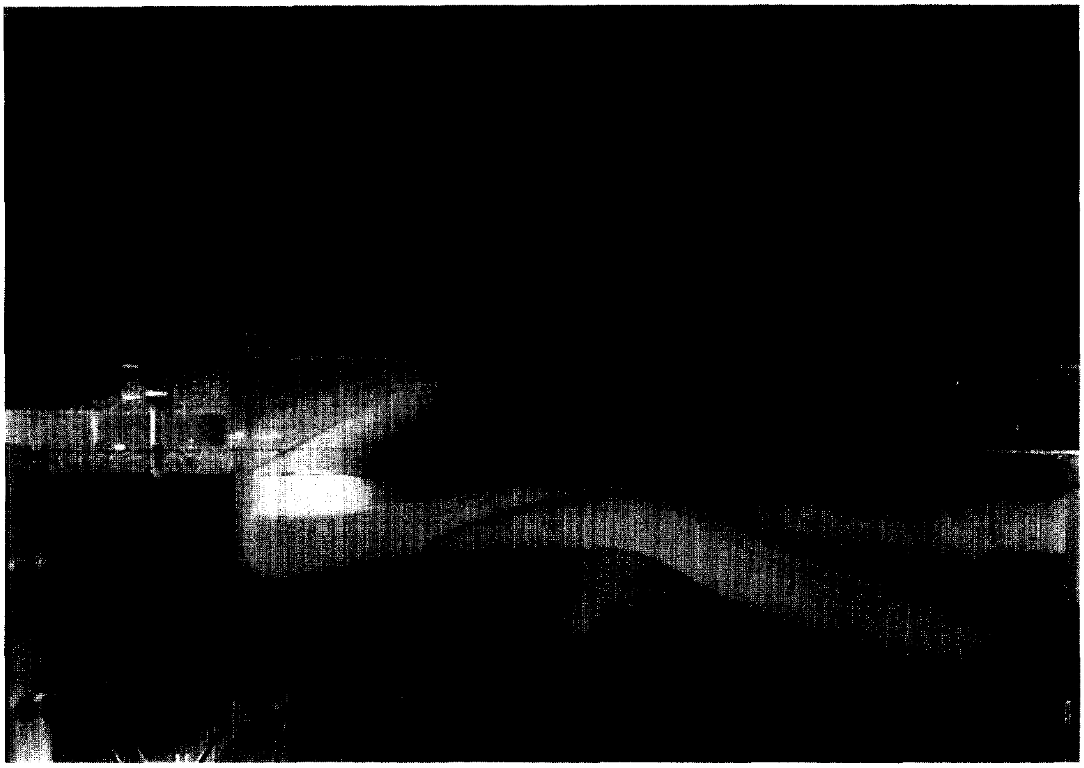

Fig. 8. Experimental photo of general view of the deformed model corresponding to stage (f) in Fig. 7.

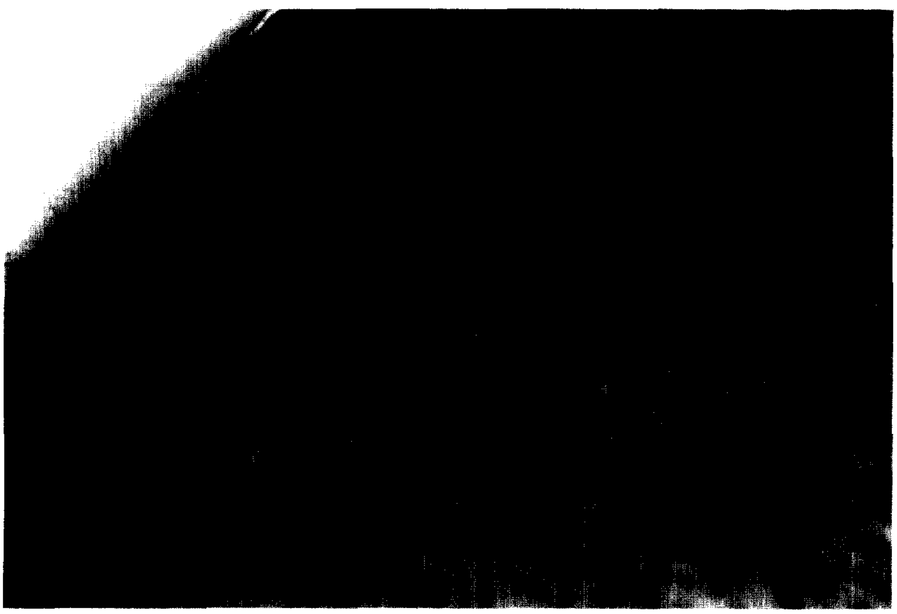

Fig. 9. Experimental photo (zoom) of area A, in Fig. 7f corresponding to the transform zone between the Luzon and Ryukyu segments of the plate boundary.

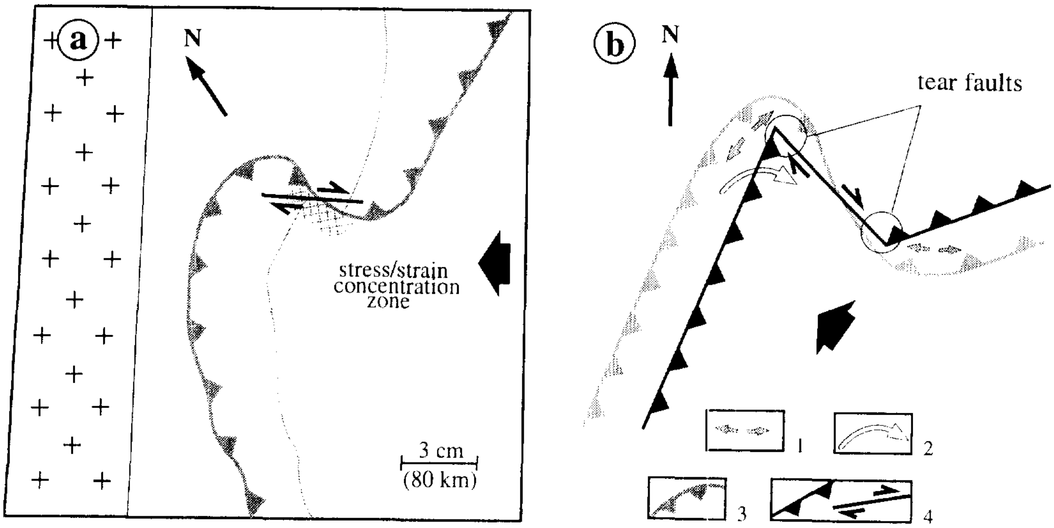

Fig. 10. Structure of the plate boundary in the transform zone between the Luzon (Taiwan) and Ryukyu segments. (a) Orientation of the transform zone at depth (solid line) corresponding to the last stage of experiment in Fig. 7f. (b) 'Subduction zone–transform fault–subduction zone' junction (simplification of (a)). *1* = extension of the upper layers of both plates near the extremities of the transform zone; *2* = rotation of the overriding corner wedge of the PSP due to shortening of this plate in the stress/strain concentration zone shown in (a); *3* = trace of the plate boundary at the surface; *4* = position of the plate boundary at depth of a few tens of kilometres (see text for more explanations).

at its most advanced stage in the northern termination of the Luzon (Taiwan) segment, where the accretionary prism is thickest and widest, and the relief is the highest (Figs. 7 and 8). Starting from the stage shown in Fig. 7d, a considerable plastic shortening of the PSP is observed along the transform zone between the Luzon and the Ryukyu boundaries, manifested by surface fracturation (Fig. 7d–f, Figs. 9 and 10a). The deep structure of the deformed model is characterized by the presence of two opposite dipping Ryukyu and Luzon 'Benioff zones' (Fig. 8). The experiment had to be stopped at the stage in Fig. 7f (also Fig. 8) because of limitations imposed by the size of the experimental installation.

6. Discussion of the experimental results

The general picture of the deformed model in Figs. 7 and 8 resembles the tectonic setting of the Luzon–Taiwan–Ryukyu area. Subduction along the Ryukyu and Luzon zones, as well as the accretion of the continental margin sediments occur as expected and do not pose any problems. What is most important is the evolution and dynamics of the transform zone. This zone (its trace at the surface) rotates clockwise during the convergence. Due to this rotation the overthrusting of the northern edge of the overriding PSP (corresponding to northern Taiwan) over the AP has a component perpendicular to the convergence vector (Figs. 7 and 10a). This effect is caused by NW plastic shortening of the PSP along the transform zone, and a NE extension of the frontal part of this plate, as shown in Fig. 10b. The extension is observed also within the AP (or more exactly, the Ryukyu Plate) along the southwestern end of the Ryukyu zone (Figs. 9 and 10b). The orientation of the transform zone, however, becomes more parallel to the convergence vector with depth, as shown in Fig. 10. Simplifying the experimental result, we obtain a classical junction, 'subduction zone–transform fault–subduction zone' (Fig. 10b). The specificity of this junction is that the subduction zones are opposite facing and so the length of the transform fault is not constant. It grows while convergence increases (see Fig. 7) due to tear failure of both plates along two tear faults shown in Fig. 10b.

The principal discrepancy between Fig. 10b (or scheme in Fig. 11a which has more realistic plate boundary geometry) and the actual situation in the Taiwan area, is that at present, there is neither sub-

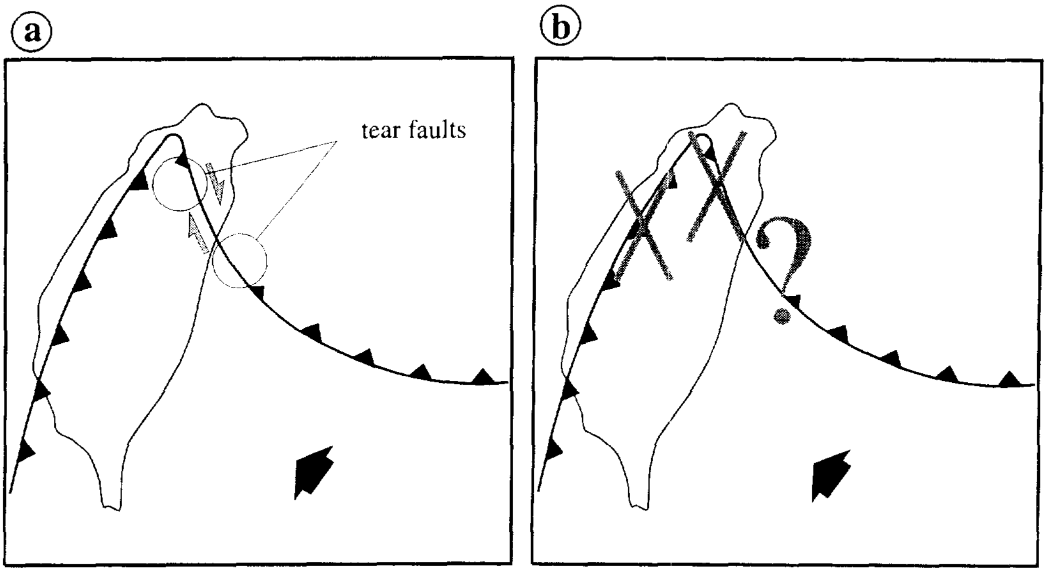

Fig. 11. Does the actual plate boundary pattern in Taiwan still correspond to the 'subduction zone–transform fault–subduction zone' junction (see text for explanations)?

duction of the AP under northern Taiwan, nor evidence of active shear faulting in (under) northern Taiwan (Fig. 11b). As mentioned above, in northwestern Taiwan there is almost no deformation, while there are clear indications of active deformation (shortening) off eastern Taiwan, especially in its northern part and further to the south along the Luzon arc. This implies that the PSP has failed offshore of northeastern Taiwan, resulting in the initiation of a new convergent plate boundary (subduction zone) as was shown by 2-D experiments (Fig. 5). We also obtained plastic shortening in this area in the 3-D experiments (see Figs. 7 and 10a), but the existing compressive stresses were not sufficient to cause complete failure of the lithosphere, as the experimental model does not include the arc (weak zone). Unfortunately, it is technically difficult to incorporate an arc (with a corresponding weakening of the plate and volcanic load) into the described 3-D experimental model. Therefore, the synthetic model developed below is based on the results of both 2-D and 3-D modelling, as well as on the available geological and geophysical data.

7. Evolutionary model for the Luzon–Taiwan–Ryukyu Plate boundary

The model is presented in Figs. 12 and 13. The first stage corresponds to intraoceanic subduction in this region (Fig. 13a). Unfortunately, there are almost no constraints on the geometry of the plate boundaries before the Luzon subduction zone arrived at the Chinese margin. What is clear is that once these two opposite subduction zones occurred (some time before the collision), the plate boundaries very rapidly assumed a form corresponding to the 'subduction zone–transform fault–subduction zone' junction presented in Fig. 10b. This type of junction is energetically very disadvantageous, and therefore unstable, as it evolves by a continuous failure of the lithosphere through the whole thickness in two tear faults. Such a process causes high normal compressive stress in the lithosphere along the transform zone, which further increases due to the subduction of the continental margin. Therefore, the lithospheric yield limit is first reached in the Luzon

Fig. 12. Evolution of the Taiwan collision in cross-section: *1* = continental (transitional) crust; *2* = sediments; *3* = oceanic crust, *4* = volcanics of the Luzon arc; *5* = core part of the overriding wedge of the PSP (fore arc block); *6* = direction of extension; *7* = zone of plastic shortening; *8* = direction of vertical movements; *9* = subduction (inset); *10* = back arc rifting (inset); *RP* = Ryukyu Plate.

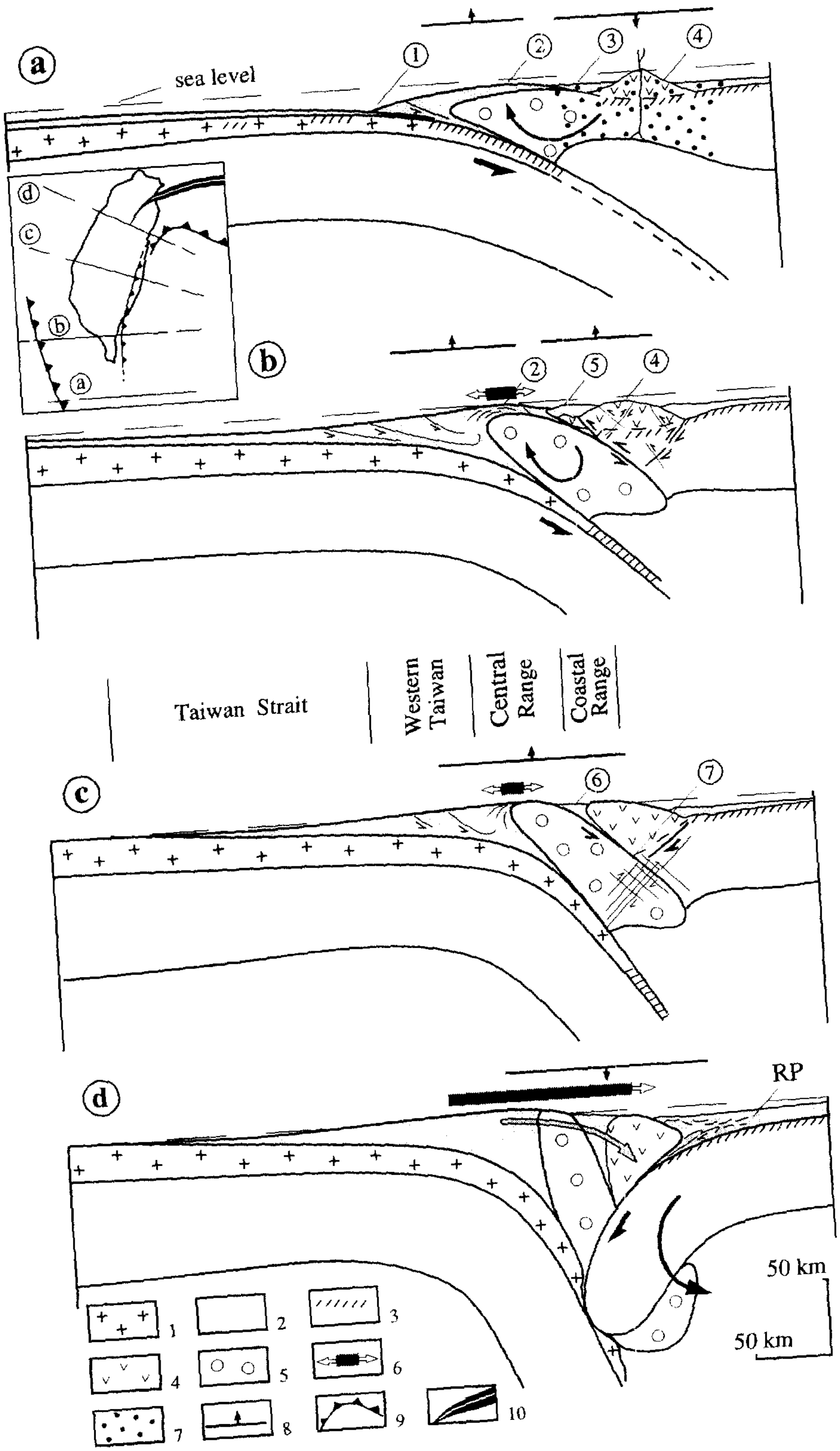

a
sea level
1
2
3
4
d
c
b
a
b
2
5
4
Taiwan Strait
Western Taiwan
Central Range
Coastal Range
c
6
7
d
RP
50 km
50 km
1
2
3
4
5
6
7
8
9
10

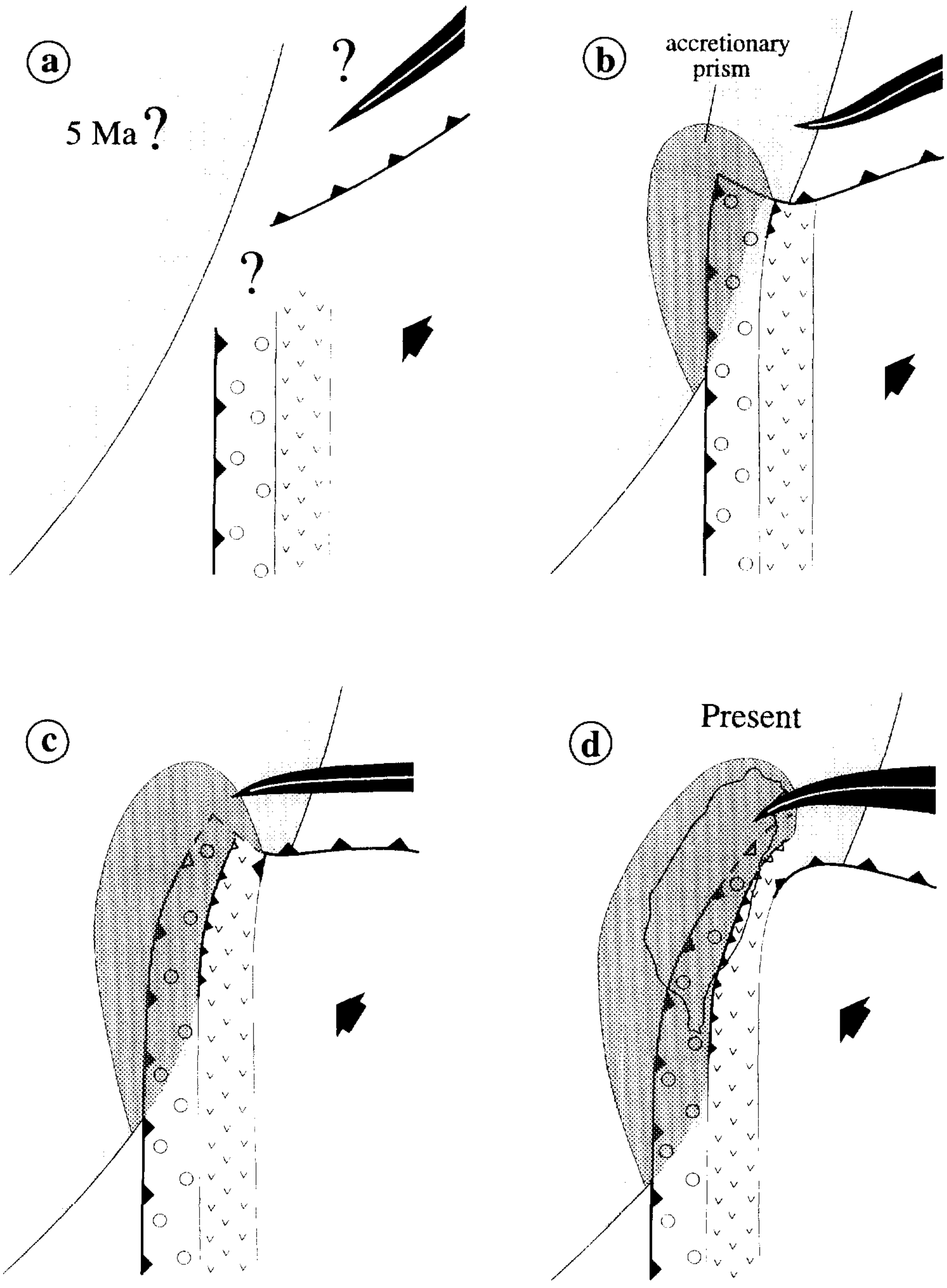

Fig. 13. Evolution of the Taiwan collision in plan (see legend of Fig. 12).

arc near the transform zone. The arc area undergoes rapid subsidence, intensive plastic shortening (Fig. 12a) and then failure (Fig. 12b). This process is followed by considerable underthrusting of the core of the PSP's frontal wedge under the arc (Fig. 12b and Fig. 13b) and some underthrusting of the PSP at the opposite side of the arc (Fig. 12b). The subducting core part of the fore arc block rotates clockwise (in cross-section), resulting in an uplift of the frontal-most (western) edge of the block, and an associated local extension and exhumation of the overlying part of the accretionary prism (Fig. 12b). The weak upper sedimentary part of the fore arc block overrides the fore arc basin and pushes sediments of the basin over the arc (Fig. 12b). The eastward underthrusting under the arc then slows down. The PSP completely fails at the opposite side of the arc, which initiates westward underthrusting of the western edge of this plate under the arc (Fig. 12c, Fig. 13c). The underthrusting PSP segment bends down, which causes rapid subsidence and a clockwise rotation (in cross-section) of the arc (formation of the subduction trench), with an extension of the upper layers of the subsiding wedge (Fig. 12d). The eastward subduction of the AP ceases. The subducting PSP collides at depth with the previously subducted AP, which causes a steeping of the PSP subduction. This effect has two consequences: a considerable non-isostatic deepening of the forming trench and a further E–W extension of the overriding orogen (northern Taiwan), associated with the subsidence of the eastern part of the orogen (Fig. 12d). The extension produced by this mechanism is rather diffuse and not intensive. It is apparently not sufficient to provide the considerable divergence required for the rifting in the Ilan Plain. This rifting is clearly associated with opening of the Okinawa trough, which seems to be independent of the Taiwan collision and might be started well before the collision (Hsu et al., 1995). The propagation of the Okinawa back arc rift to the southwest was blocked with the initiation of collision, which resulted in a high compression of the AP, especially along the transform zone with two tear faults. This compression was released only after the failure of the PSP offshore of northeastern Taiwan and the initiation of subduction of this plate, some 1 Ma ago (Fig. 13c). The tear faults no longer exist and the initiating subduction under northeastern Taiwan is becoming a part (southwestern continuation) of the Ryukyu subduction. Moreover, the whole northeastern segment of the Taiwan plate boundary becomes a part of the southwestward-propagating Ryukyu arc–back arc system (Fig. 14).

8. Comparison of the model to the observations

Information about the Taiwan collision is certainly insufficient to reconstruct the evolution of this complex process in a way which would satisfy all the researchers working on Taiwan geology and geophysics. That is why there are many different approaches and schemes explaining the various stages and elements of the collision, which do not agree with each other, so that the creation of a synthetic model, based only on the observations, is a quite hard task. Our model is based on first-order mechanics of the lithosphere in a subduction/collision environment roughly corresponding to the Taiwan area. Therefore this model cannot pretend to explain all details of the geological evolution and deep structure of this region. On the other hand, the available data allow us to test some of the principal model predictions. We will start this analysis with the offshore area of southern Taiwan, which corresponds to the beginning of collision. The first prediction of the model is that the initiation of subduction of the continental margin causes a rapid flexural subsidence of the Luzon arc (Fig. 12a). Such subsidence is corroborated by the stratigraphic records in the Coastal Range (Dorsey, 1992; Chang and Chi, 1983). Second, at this stage, and later in time (or further to the north), the arc area undergoes considerable shortening (Fig. 12b). Such a shortening is indeed revealed by the GPS measurements (Fig. 2a) and is manifested by the intensive seismicity in the arc area near southern Taiwan (Fig. 2b). Third, the shortening is accompanied by the formation of a lithospheric east-dipping thrust fault (Fig. 12b, Fig. 13b). Such a fault corresponds well to the Longitudinal Valley Fault (see Fig. 1). A displacement along this fault results in a closure of the fore arc basin (the Luzon trough) with the formation of a suture zone, the Longitudinal Valley. On the other hand, thrusting along the Longitudinal Valley Fault causes an uplift of the western margin of the Luzon arc, which makes up the Coastal Range of Taiwan (Fig. 12c). Fourth, a rotation of the subducting core of the fore arc block results in the uplifting of its western edge, and in a local extension of the overlying accreted sediments (Fig. 12b). Such an extension is revealed by GPS data for the southern part of the Central Range (Yu et al., 1995) (see also Fig. 2a). Further to the north the progressive extension and uplift become more localized (Fig. 12c). In combination with erosion, they cause the exhumation of ever deeper rocks along the eastern margin of the Central Range

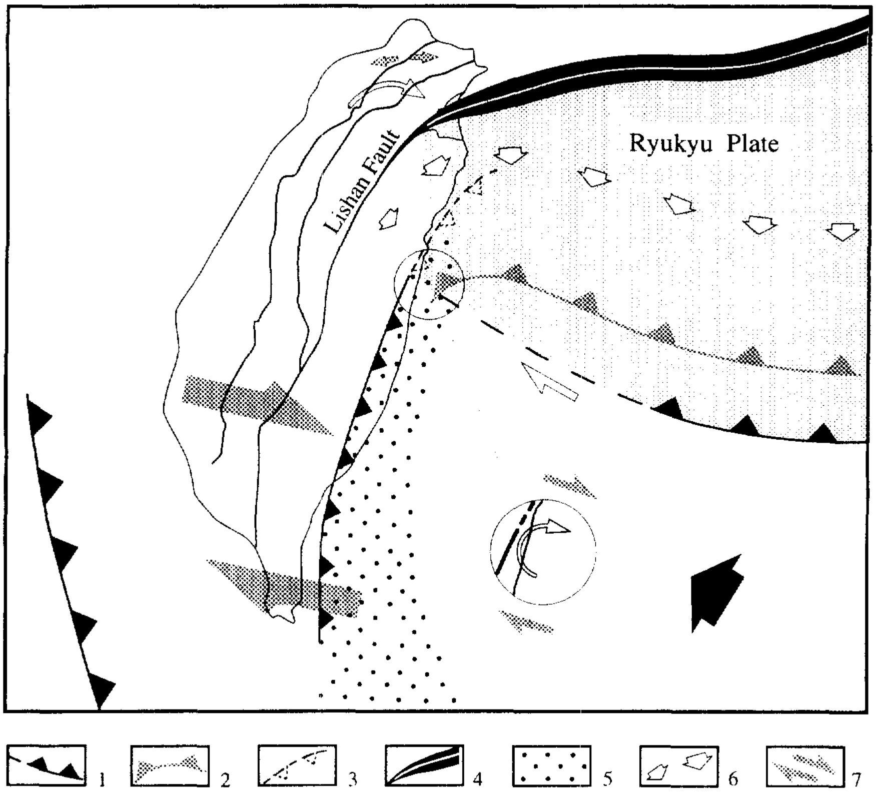

Fig. 14. Present-day plate boundaries and large-scale deformation pattern: *1* = trace of plate boundary at the surface; *2* = schematic position of the plate boundary at several kilometres depth; *3* = dead plate boundary; *4* = axis of back arc rifting; *5* = diffused plastic shortening zone; *6* = motion direction of the Ryukyu Plate sucked to the retreating Philippine Sea subducting plate; *7* = direction of the diffused shear.

(Tananao complex), with a syn-collisional exhumation depth in excess of 10 km (Wang Lee et al., 1982; Ernst, 1983). The underthrusting of the fore arc block is then blocked, with lithospheric failure occurring at the eastern margin of the Luzon arc along northern Taiwan. The model predicts the initiation of westward subduction of the PSP in this region (Fig. 12d, Fig. 13c, d), which takes up almost the entire rapid convergence between the AP and the PSP. There are several sets of arguments in favour of such a subduction. First is the cessation of subduction of the AP under northern Taiwan, revealed by the GPS data (Fig. 2a). Second is the existence of an intense gravity minimum along the northeastern Taiwan margin (Fig. 2c), caused (according to the model) by a sharp down-bending of the PSP underthrusting along an angular-shaped boundary. The bending also results in subsidence below sea level of the Coastal Range which now makes up part of the inner slope of the forming depression (trench). This depression has no bathymetric expression as it is filled with sediments (shed from the rapidly eroding orogen), forming a sedimentary basin. A basin in this area was indeed recently revealed by multichannel seismic profiling (Lallemand et al., 1995). In fact, there are two superimposed basins. The lower (older) Suao basin is intensively deformed along a sequence of NW-dipping thrusts and NE–SW-trending folds. The NW–SE shortening was accompanied by very rapid differential subsidence of the basin, which resulted in the formation of the upper (Hoping) basin. The age of the deformation and subsidence is unknown. According to our model this event corresponds to the failure of the PSP and the initiation of NW-ward subduction under northern Taiwan (Fig. 13c).

It should be noted that the formation of a subduction zone (the failure of the lithosphere corresponding to the stage shown in Fig. 12c and Fig. 13c) involves deformation and thickening of the crustal layer, which can be scrapped from the mantle base, forming a topographic high instead of a depression (Shemenda, 1994). The depression (trench) forms later, after a complete failure of the lithosphere and the initiation of subduction due to the bending of the subducting plate. Therefore one cannot expect a simple structure or dynamics of the sedimentary and crustal layers in the incipient subduction zone especially near its youngest southern termination.

The third argument which supports subduction of the PSP under northeastern Taiwan seems to be provided by seismological data. A supposed subduction zone is associated with a concentration of seismicity (Fig. 2b) and with a high-velocity zone observed to a depth of at least 80 km (Rau and Wu, 1995). Vertical seismicity sections through this zone do not reveal the geometry of a subducted plate (Fig. 3). The seismicity is diffuse, which implies considerable plastic deformation in the corner zone near northeastern Taiwan. Nevertheless, section A–A′ in Fig. 3 displays a west-dipping swarm of earthquakes which may correspond to the subducted PSP. The swarm gradually disappears to the south (sections B–B′, C–C′ and D–D′ in Fig. 3). Horizontal seismicity sections deeper than 70 km (up to near 150 km) clearly outline the PSP, subducted in the Ryukyu zone (Fig. 15). Shallower sections again show a diffuse deformation. Nevertheless, a majority of the hypocentres at these depths can still be accommodated within comparatively narrow strips (shaded in Fig. 15). These strips bend to the south along the northeastern margin of Taiwan. We interpret them as corresponding to the PSP, subducted along an angular-shaped boundary, including the Ryukyu subduction zone and the incipient subduction zone along northeastern Taiwan (Fig. 16).

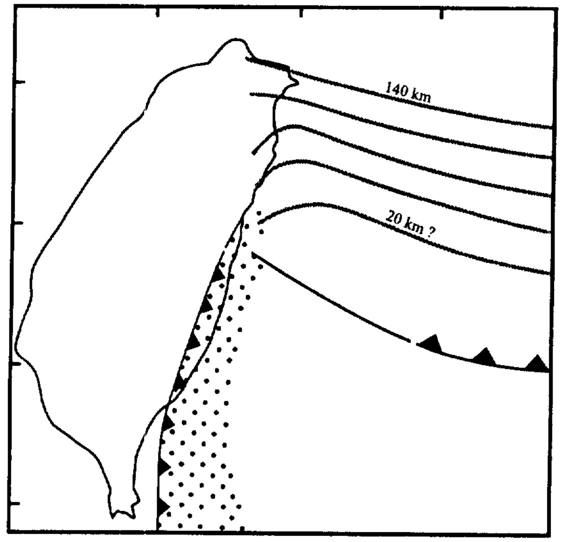

Fig. 16. Principal scheme of counters of the Benioff zone (shaded lines) corresponding to the subducted PSP (symbols as in Fig. 14).

A fourth argument is that the extension and rifting observed in northern Taiwan (see Fig. 2a and Fig. 14) would not be possible without a release of compres-

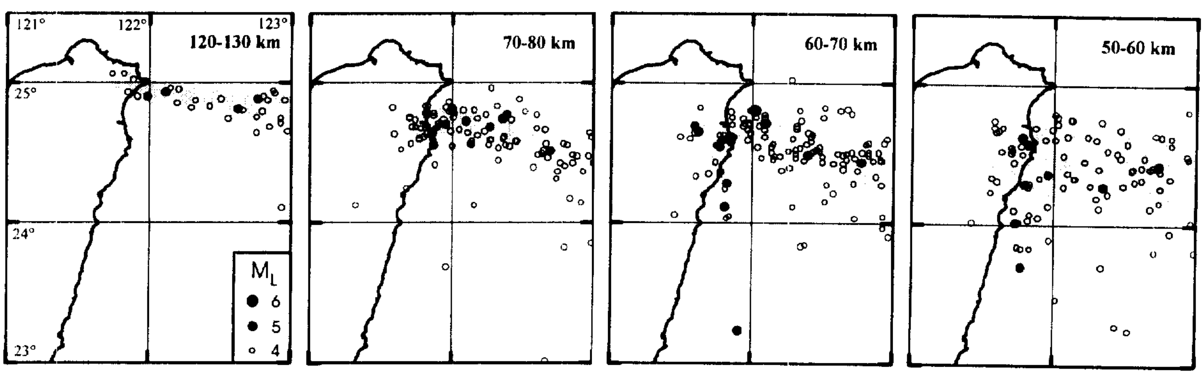

Fig. 15. Horizontal seismicity sections: projections on the horizontal plain of the hypocentres from 50 to 60 km, 60 to 70 km, 70 to 80 km and 120 to 130 km for earthquakes with magnitude $M_L \geq 4$ located during 1973 to 1995 by the TTSN. Seismicity concentration zones are shaded.

sive stresses, caused by the failure of the PSP, and accommodation of convergence between the AP and PSP in the incipient subduction zone. This zone becomes a continuation of the southeastward-retreating Ryukyu subduction zone, which allows the Okinawa rift to propagate into Taiwan. The extension (rifting) is localized along a pre-existing weak zone, the Lishan Fault (Fig. 14). Thus southward-propagating incipient subduction and rifting, as well as the whole of northeastern Taiwan, become a part of the Ryukyu–Okinawa subduction system. A similar conclusion was made by Teng (1995).

Finally, the present plate boundary pattern (Fig. 14) implies some overlapping of two opposite-dipping lithospheric thrust (subduction) faults corresponding to the dying Longitudinal Valley Fault and southward-propagating Ryukyu subduction. The overlapping zone (which in whole propagates southwards) must undergo a clockwise rotation (in plan) and/or a right-lateral diffusive shear, as shown in the inset to Fig. 14. Such a deformation is corroborated by the GPS data (see Fig. 2a). The latitude of the mentioned rotation zone approximately coincides with that of the southern extremities of both the seismicity concentration and the gravity minimum along the northeastern margin of Taiwan (see shaded horizontal dashed line throughout Fig. 2). All these correspond to the PSP failure front or to the tip of the southward-propagating Ryukyu subduction zone.

9. Conclusions

Taiwan represents one of the few examples of an active arc–continent collision or more exactly, of subduction of the continental margin (continental subduction) which follows oceanic subduction and the formation of a volcanic arc. The collision is oblique and therefore propagating, which provides us with a unique opportunity to study the different evolutionary stages of this process, and to understand what an arc–continent collision really means in terms of lithospheric mechanics. Our conclusion is that it means first of all a deformation (plastic shortening) and a failure of the overriding plate in the arc area (the Luzon arc), which is a weak zone. The deformation occurs due to compression of this plate growing with the continental margin subduction. The shortening of the Luzon arc carried by the Philippine Sea Plate (PSP) is followed by a failure of this plate which occurs first at the western side of the arc along the eastward-dipping fault, the Longitudinal Valley Fault. The most rigid (core) part of the overriding PSP wedge underthrusts the arc along this fault, while the soft upper sedimentary layers of the wedge override and 'collide' with the fore arc basin. This process results in a closure of the fore arc basin and an uplifting of this whole area. The uplift occurs due to both the thickening of the accretionary structure of the forming orogen and the continuing subduction under it of a progressively thicker Asian crust. In the model (Fig. 12) we assumed that the accreted series are only sedimentary and volcanic complexes. In fact, the subducting Asian crust may also be involved in this process by its thrusting and/or buckling (Chemenda, 1995). Underthrusting of the PSP's frontal wedge is then blocked, and the PSP fails at the opposite side of the Luzon arc accreted to (overthrusted) the orogen. The failure results in the initiation of southward-propagating subduction of the PSP under northeastern Taiwan. Further evolution of northern Taiwan is greatly affected by the neighbouring Ryukyu subduction system which is peculiar to the Taiwan collision. This zone retreats to the southeast, causing the opening of the Okinawa trough, a typical back arc rift. The western limit of the rift was the Taiwan orogen associated with the strong compression of the Asian Plate. The failure of the PSP offshore of northeastern Taiwan, some 1 Ma ago, released the compression. The incipient subduction zone forming after this failure, is becoming part of the southeastward-retreating Ryukyu subduction zone. The Okinawa rift thus acquires the ability to propagate into Taiwan along a pre-existent weak zone, the Lishan Fault (Fig. 14).

To summarize, the arc–continent collision in Taiwan includes the following sequence of major processes in time, or from the south to north: (1) NW shortening of the PSP in the Luzon arc; (2) failure of this plate at the western side of the arc, with the formation of the eastward-dipping Longitudinal Valley Fault (the transient plate boundary); (3) closure of the fore arc basin and a rapid uplift of the orogen; (4) failure of the PSP at the eastern side of the Luzon arc partly overthrusted the orogen, and the initiation of subduction of the PSP under northeastern Taiwan; (5) 'back arc' rifting in the rear of this incipient subduction zone (in northern Taiwan). All these processes commence with some delay with respect to the preceding one and propagate southwards.

Acknowledgements

We thank S. Lallemand and J.-F. Stephan for the useful discussions, R.D. Hwang for plotting the seismicity sections, S.B. Yu for providing an updated GPS data map and Y. Font for the idea of using horizontal seismicity sections.

References

Angelier, J., et al., 1995. Crustal extension in active orogen: Taiwan. In: Sino–French Symposium Active Collision in Taiwan, Taiwan, pp. 25–32.

Barrier, E. and Angelier, J., 1986. Active collision in eastern Taiwan, Coastal Range. Mem. Geol. Soc. China, 7: 135–155.

Biq, C.C., 1972. Transcurrent buckling, transform faulting and transpression, their relevance in eastern Taiwan kinematics. Pet. Geol. Taiwan, 20: 1–39.

Chai, B.H., 1972. Structure and tectonic evolution of Taiwan. Am. J. Sci., 272: 389–432.

Chang, L.S. and Chi, W.R., 1983. Neogene nannoplankton biostratigraphy in Taiwan and the tectonic implications. Pet. Geol. Taiwan, 19: 93–141.

Chemenda, A.I., 1995. Evolutionary model for the Taiwan collision explaining rock exhumation and extension in the Central Range. In: Sino–French Symposium Active Collision in Taiwan, Taiwan, pp. 41–48.

Chemenda, A.I., Mattauer, M., Malavieille, J. and Bokun, A.N., 1995. A mechanism for syn-collisional deep rock exhumation and associated normal faulting: results from physical modeling. Earth Planet. Sci. Lett., 132: 225–232.

Chemenda, A.I., Mattauer, M. and Bokun, A.N., 1996. Continental subduction and a mechanism for exhumation of high-pressure metamorphic rocks: new modelling and field data from Oman. Earth Planet. Sci. Lett., 143: 173–1822.

Cheng, S.-N., Yeh, Y.-T. and Lee, C.-T., 1995. A stress map in Taiwan. In: Sino–French Symposium Active Collision in Taiwan, Taiwan, pp. 57–69.

Chi, W.R., Namson, J. and Suppe, J., 1981. Stratigraphic record of plate interactions in the Coastal Range of eastern Taiwan. Mem. Geol. Soc. China, 4: 155–194.

Crespi, J., 1995. Deformation partitioning at shallow crustal levels in the Taiwan arc–continent collision. In: Sino–French Symposium Active Collision in Taiwan, Taiwan, pp. 71–76.

Ernst, W.G., 1983. Mountain building and metamorphism: a case history from Taiwan. In: K.J. Hsu (Editor), Mountain Building Process. Academic Press, London, pp. 247–256.

Dorsey, R.J., 1992. Collapse of the Luzon volcanic arc during onset of arc continent collision: evidence from a Miocene–Pliocene unconformity, eastern Taiwan. Tectonics, 11: 177–191.

Ho, C.S., 1986. A synthesis of the geologic evolution of Taiwan. Tectonophysics, 125: 1–16.

Ho, C.S., 1988. An introduction to the geology of Taiwan: explanatory text of the geologic map of Taiwan (2nd ed.). Ministry of Economic Affairs, R.O.C., 164 pp.

Hsu, S., Sibuet, J.-C., Shu, C.-T. and Liu, C.-S., 1995. Decoupling of back arc extension from arc–arc collision. In: Sino–French Symposium Active Collision in Taiwan, Taiwan, pp. 131–140.

Karig, D.E., 1973. Plate convergence between the Philippine and the Ryukyu Islands. Mar. Geol., 14: 153–168.

Lallemand, S., Liu, C.-S. and Lin, S.-J., 1995. Behaviour of the Ryukyu fore arc sliver in the wake of the indenting northern Luzon arc (east of Taiwan). In: Sino–French Symposium Active Collision in Taiwan, Taiwan, pp. 167–175.

Letouzey, J. and Kimura, M., 1986. The Okinawa Trough: genesis of a back-arc basin developing along a continental margin. Tectonophysics, 125: 209–230.

Lewis, S.D. and Hayes, D.E., 1983. The tectonics of northward propagating subduction along eastern Luzon, Philippine Islands. Geophys. Monogr., 27: 56–78.

Lundberg, N., Reed, D.L. and Liu, C.H., 1991. The submarine propagating tip of the Taiwan collision: shallow crustal structure and orogenic sedimentation. Taicrust Workshop Proc., Taipei, pp. 93–102.

Lundberg, N., Reed, D.L., Liu, C.-S., Chen, M.-P. and Gerace, D.A., 1995. Fore arc basin closure and orogenic sedimentation in the submarine suture zone south of Taiwan: response to arcward transfer of plate convergence. In: Sino–French Symposium Active Collision in Taiwan, Taiwan, pp. 243–262.

Murphy, R.W., 1973. The Manila Trench–west Taiwan fold belt: a flipped subduction zone. Geol. Soc. Malaysia Bull., 6: 27–42.

Page, B.M. and Suppe, J., 1981. The Pliocene Lichi melange of Taiwan: its plate tectonic and olistostromal origin. Am. J. Sci., 281: 193–227.

Pelletier, B. and Stephan, J.-F., 1986. Middle Miocene obduction and Late Miocene beginning of collision registrated in the Hengchun peninsula: geodynamic implications for the evolution of Taiwan. Tectonophysics, 125: 133–160.

Rau, R.-J. and Wu, F.T., 1995. Tomographic imaging of lithospheric structures under Taiwan. Earth Planet. Sci. Lett., 133: 517–532.

Seno, T., 1977. The instantaneous rotation vector of the Philippine Sea plate relative to the Eurasian plate. Tectonophysics, 42: 209–226.

Shemenda, A.I., 1993. Subduction of the lithosphere and back arc dynamics: insights from physical modeling. J. Geophys. Res., 98: 16167–16185.

Shemenda, A.I., 1994. Subduction: Insights from Physical Modeling. Kluwer, Dordrecht, 215 pp.

Shemenda, A.I., Hsieh, C.-H. and Yang, R.K., 1992. Reversal subduction and a geodynamic model of the collision in Taiwan. Acta Geol. Taiwan., Sci. Rep. NTU, 30: 101–104.

Sibuet, J.-C., 1991. The southern Okinawa trough. In: TAICRUST Workshop Proceedings, Taipei, pp. 117–126.

Suppe, J., 1981. Mechanics of mountain building and metamorphism in Taiwan. Mem. Geol. Soc. China, 4: 67–89.

Suppe, J., 1984. Kinematics of arc–continent collision, flipping of subduction, and back arc spreading near Taiwan. Mem. Geol. Soc. China, 6: 21–24.

Teng, L.S., 1990. Geotectonic evolution of late Cenozoic arc–continent collision in Taiwan. Tectonophysics, 183: 57–76.

Teng, L.S., 1995. Neotectonics of northern Taiwan and southern Ryukyu. In: Sino–French Symposium Active Collision in Taiwan, Taiwan, pp. 287–292.

Wang, C. et al., 1994. A sturdy of seismicity distribution in north-eastern Taiwan. In: Proc. 5th Taiwan Geophys. Symp., Taiwan, pp. 421–430.

Wang Lee, C., Wang, Y., Yen, T.P. and Lo, C.H., 1982. Polymetamorphism in some gneiss bodies, Hoping–Chipan area, Hualien, eastern Taiwan. Acta Geol. Taiwan., 23: 122–139.

Wu, F.T., 1978. Recent tectonics of Taiwan. J. Phys. Earth., Suppl., 26: S265–S299.

Yeh, Y.H. and Yen, H.Y., 1991. Gravity anomalies of Taiwan and their tectonic implication. Taicrust Workshop Proc., Taipei, pp. 175–184.

Yu, S.-B., Chen, H.-Y. and Kuo, L.-C., 1995. Velocity field of GPS stations in the Taiwan area. In: Sino–French Symposium Active Collision in Taiwan, Taiwan, pp. 317–327.